



Increasing model structural complexity inhibits the growth of initial condition errors

Mark E. Baird^{a,*}, Iain M. Suthers^b

^a School of Mathematics and Statistics, University of NSW, Sydney, NSW 2052, Australia

^b School of Biological, Earth and Environmental Sciences, University of NSW, Sydney, NSW 2052, Australia

ARTICLE INFO

Article history:

Received 4 December 2008

Received in revised form 12 November 2009

Accepted 3 December 2009

Available online 12 January 2010

Keywords:

Initial conditions

Structural complexity

Pelagic ecosystem

Ensemble spread

Non-linear dynamics

Predictive skill

ABSTRACT

One source of inaccuracy in non-linear deterministic ecological models is the growth of initial condition errors. A size-resolved pelagic ecosystem model is used to investigate the effects of changing model structural complexity on the growth rate of initial condition errors. Structural complexity is altered by (1) changing the number of biological size-classes; and (2) changing prey size-ranges which changes the number of linkages for the same number of size-classes. Ensembles of model runs with tiny variations in initial conditions are undertaken and member divergence used to estimate ensemble spread (a measure of the growth of initial condition errors). Increasing prey ranges and therefore the number of linkages greatly reduced the rate of growth of initial condition errors, but ecosystem behaviour is also altered, restricting the generality of the result. At more than 123 size-classes, increasing the number of size-classes while not changing either the model equations or parameters does not alter ecosystem behaviour for over 200 days. In this case, increasing structural complexity through increasing the number of size-classes did not alter the growth of initial condition errors for the first 30 days of the simulations, but afterwards reduced error growth. There are many advantages of parsimonious ecological models with small numbers of classes and linkages, but they are more likely to suffer from the growth of initial condition errors than structurally complex models.

© 2009 Elsevier B.V. All rights reserved.

1. Introduction

The goal to predict the future state of a natural system from a set of initial conditions has become a common pursuit in the physical and life sciences. Since the realisation of the non-linear behaviour of physical (Lorenz, 1963) and ecological (May, 1973) systems, it has been recognised that there are fundamental limits to prediction by non-linear mathematical models (Huisman and Weissing, 2001; Melbourne and Hastings, 2009). One limit relates to the divergence of model predictions from near-identical states due to non-linear interactions.

For a simple deterministic model of convection in a rotating flow with small errors in initial conditions, Lorenz (1968) showed that after a short period the divergence of model state is independent of the magnitude of initial conditions errors. This finding later gave rise to the description of the “butterfly effect” (Hilborn, 2004), and implies that for some systems no level of precision in specifying of initial conditions can avoid errors in model predictions. This paper investigates the phenomena of growth of initial condition errors in a pelagic ecosystem model, and

in particular, how error growth changes with the structural complexity of the model.

The effect of model structural complexity on population dynamics has been studied extensively. The majority of authors have concentrated on the global behaviour of models. For example there are a large number of studies on the effect of model structural complexity on population stability (May, 1973; Duffy et al., 2007) and dynamics (Fussmann and Heber, 2002; Rai et al., 2007). Early studies suggested that complexity increased stability (MacArthur, 1955), but a more complicated consensus has been found (May, 1973). Tilman (1999) summarised the consensus by stating for the case of diversity as a source of structural complexity, that diversity stabilises community structure, but destabilises the dynamics of individuals.

In an investigation into the effect of initial condition sensitivity on predicting outbreaks of gypsy moths, Wilder (2001) found that even when it is assumed that the model perfectly reflects the population dynamics and that the parameters are known exactly, extremely small errors in the specification of initial conditions are required to obtain reliable predictions for less than a decade. While similar initial condition experiments on other ecological models are rare, studies of the effects perturbations from a stable state, or transients, have been undertaken (Hastings, 2004), and may shed light on initial condition problems.

* Corresponding author. Tel.: +61 416 631 657; fax: +61 3 6232 5000.
E-mail address: m.baird@unsw.edu.au (M.E. Baird).

Chen and Cohen (2001) investigated the effect of food web complexity on transient behaviour in a predator–prey type ecosystem. They found that given a fixed level of connectance the size and duration of transient responses to perturbations increase with the number of species. Given a fixed number of species, as connectance increases, the size and duration of transient responses to perturbations may increase or decrease depending on the type of link that is varied. The experiments of Chen and Cohen (2001) give useful insight into initial condition errors (initial condition errors could be considered a type of transient). However, their emphasis was on a shift in ecosystem behaviour due to a relatively large transient from an equilibrium state, rather than the spread of trajectories due to small changes in initial conditions. Given the importance of initial condition error growth in deterministic ecological models, more focused work on what determines the rate of initial condition error growth is warranted.

A recently developed size-resolved pelagic ecosystem model (Baird and Suthers, 2007) has been designed in such a way that it may provide additional insights to these earlier studies. The model is constructed from process descriptions that are based on plankton size. The size dependence includes physical limits on ecological processes, such as projected area of a phytoplankton cell limiting the amount of light that can be absorbed. Size also determines physiological rates such as maximum growth rates as determined using allometric relationships. By using this size-dependence in model construction, the number of biological classes in the Baird and Suthers (2007) model can be changed without changing the underlying equations or the parameter values. This is achieved by using the same model equations for all size-classes within a functional group (phytoplankton, protozoans and metazoans), and all coefficients in these equations being determined from allometric relationships. The independence of number of size-classes was illustrated in numerical experiments that showed that as model resolution is increased, the model output converges on a solution (Baird and Suthers, 2007). Or more precisely, diverges from an initial state later with greater resolution. Additionally, in the size-resolved model, the number of interactions per size-class can be varied by changing one parameter, the maximum size difference of predators and prey.

This paper uses the size-resolved pelagic ecosystem model to investigate the effect of model structural complexity on the growth of initial condition errors. Numerical experiments are undertaken for sufficiently small initial condition perturbations that the divergence of trajectories is independent of the magnitude of the initial condition errors (Lorenz, 1968; Baird, in press). Experiments include varying the number of size-classes by 2^5 , and the maximum size difference between predators and prey by a factor of 8. From the results of the experiments, a discussion is undertaken of the impacts of initial condition errors on pelagic ecosystem models, and more generally on predator–prey models, and the means for minimising their growth in modelling studies considered.

2. Model description

The size-resolved pelagic ecosystem model contains three functional groups: phytoplankton, protozoans and metazoans – requiring three separately resolved size distributions. Four features of the size-resolved model are of particular interest to the modelling of pelagic ecosystems: (1) physical descriptions of planktonic interactions are used to explicitly represent the size-dependencies of limiting physical processes to ecological interactions. Physical descriptions include, for example, calculating the encounter rates of predators and prey based on the physical properties of the fluid and the geometric properties of the organism (Jackson, 1995); (2) physiological rates are calculated

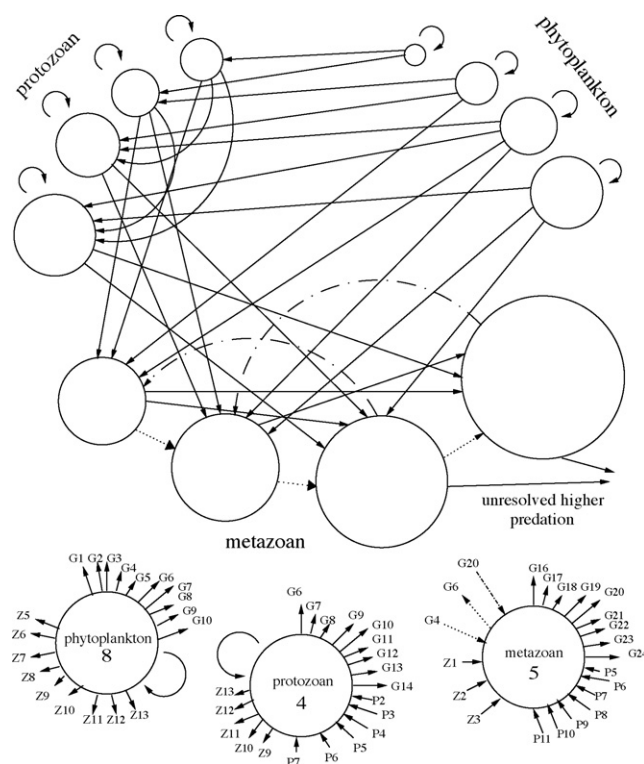


Fig. 1. Schematic of the size-resolved pelagic ecosystem model. The phytoplankton and protozoan groups divide, as represented by the arrow turned on itself. Growth of individuals between metazoan size-classes is represented by dashed arrows, while spawning of eggs by metazoa is represented by dot-dashed lines. All other lines are predation terms. In the top schematic, predation is limited to just two size-classes of predators within each functional group, although the 62 size-class configuration typically has 9–11. In the lower schematic, all interactions are given for the 8th phytoplankton class, 4th protozoan class and the 5th metazoan class in the 62 size-class configuration. The largest 15 metazoans have unresolved loss terms which are modelled implicitly using a quadratic loss term that returns nitrogen to the dissolved inorganic nitrogen pool.

from allometric relationships found in the literature; (3) a distinction is made in the model between animals that reproduce through division, the protozoa, and those that grow between different life stages, the metazoa (Figs. 1 and 2); and (4) the interaction of predators and prey is based on size rather than an *a priori* trophic structure.

A biological configuration is used composed of 62 size-classes doubling in biomass between classes and ranging in volume over 19 orders of magnitude from $0.32 \mu\text{m}^3$, representative of the cyanobacteria *Prochlorococcus* sp., to $2.05 \times 10^{18} \mu\text{m}^3$, representative of a metazoan size-class with an equivalent spherical radius of 78.8 cm. The phytoplankton size-classes extend through the first 17 size-classes, protozoan from the 9th to 21st, and metazoan from the 18th to 62nd.

In this paper, model resolution is altered by repetitively halving or doubling the interval between size-classes. The smallest and largest size-classes for each functional group remains the same (Fig. 3). The model equations, and the allometric relationships from which physiological rates are determined, are unchanged by model resolution. This paper details new results from the 17, 32, 62, 123 and 245 size-class configurations that were used in Baird and Suthers (2007), and the first results from the more highly resolved 489 size-class configuration. These configurations represent an increase in mass between size-classes of a factor of 2^4 , 2^2 , 2^1 , $2^{1/2}$, $2^{1/4}$ and $2^{1/8}$ respectively (Fig. 3).

The most sensitive parameters in the 62 size-class configuration are the size range of prey for each predator. In the model

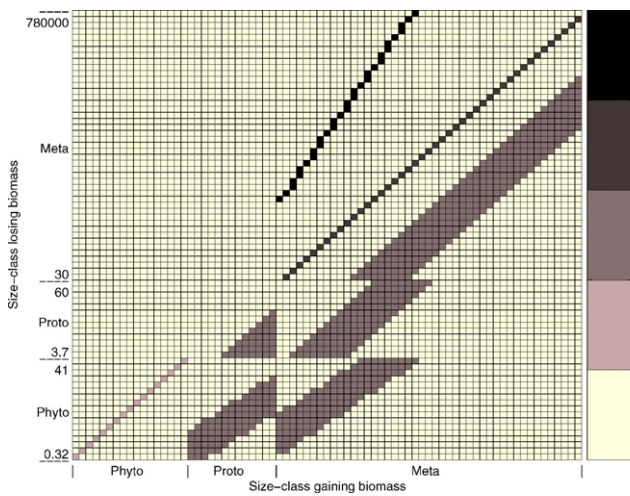


Fig. 2. Schematic of the processes linking size-classes in the 62 size-class configuration with unaltered maximum size ratios between predators and prey. The x-axis gives the size-class gaining biomass, and the y-axis the size-class losing biomass. Processes resolved are phytoplankton growth (photosynthesis), grazing, individual growth by metazoans and egg spawning by metazoans. White boxes represent no direct link between size-classes. In the case of phytoplankton growth the mass lost is from internal reserves at that size-class. Spawning appears in the top left half of the square as it is a transfer of biomass to smaller size-classes. Photosynthesis appears on the 1:1 line, as biomass is not transfer. Grazing and individual growth appear in the bottom right half as they move biomass to larger size-classes. Mortality terms on the largest metazoans due to unresolved predators are not included (as they are considered a boundary condition).

results presented here, metazoans feed on plankton with an equivalent spherical radius of 10.26–90.73 times smaller than themselves, while the range for protozoans is 3.0–22.6. These predator–prey ratios are then varied by factors of 0.5, 1 (unaltered), 2, 3, and 4. Neither protozoans or metazoans have prey preference other than size limits and a size-dependent rate of encounter. The interactions between size-classes in the 62 size-class configuration with these predator–prey ranges have been qualitatively represented in Fig. 1. Mass moves between size classes based on growth of the phytoplankton population (creating organic matter from

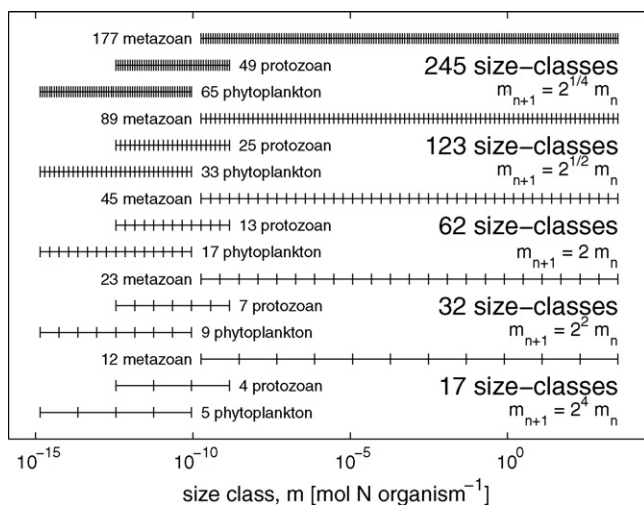


Fig. 3. The biological size-classes for five different resolution configurations. The boundaries of the phytoplankton, protozoan and metazoan grids are identical for all configurations, while the gap between classes is halved with each increase in grid resolution. The 17 and 32 size-classes grids are nominally 17 and 32 size-classes, as the mismatch between size-classes on the metazoan and protozoan grids (a result of requiring that the grids in the different resolutions all have the same boundaries) produces organisms at 18 and 33 size-classes respectively. The 489 size-class configuration (not shown) increases by 2^{1/8} each size-class, and has 129 phytoplankton, 97 protozoans and 353 metazoans.

inorganic constituents), grazing by protozoans and metazoans, growth of individual metazoans from one size-class to another, and the spawning of eggs by metazoans. Note that of the 75² = 5625 possible interactions between size classes, only 725 have a process (Fig. 2). For more details, the reader is referred to Baird and Suthers (2007).

The size-resolved model is coupled to a 1D model of the oceanic mixed layer. The vertical profiles for vertical diffusivity, turbulent dissipation rate, solar radiation and wind-driven velocity over a four day period (200 days after the simulation begins) are given in Fig. 1 of Baird and Suthers (2007). The wind-driven velocity induces a velocity shear that affects the calculation of the turbulence state variables such as vertical diffusivity and turbulent dissipation rate, but there is no advection in the model.

3. Experimental design

To investigate the effect of the number of size-classes on the growth of initial condition errors, ensembles of 22, 40, 76, 76, 76, and 489 size-class configurations respectively (Fig. 3). For the 17, 32 and 62 size-class configurations, each ensemble is composed of a control run, and a perturbed member for each state variable. As there is an overlap in the phytoplankton, protozoan and metazoan size-ranges, the ensembles consist of 21, 39 and 75 perturbed members for the 17, 32 and 62 size-class configurations respectively. The initial condition of the perturbed state variable is increased by a magnitude of 1/2,480,000 of the total concentration of organic nitrogen, while all other state variables are kept constant.

For the 123, 245 and 489 configurations, the initial perturbation is of the same magnitude, but divided evenly over 2, 4 and 8 consecutive size-classes respectively, resulting in 76 member ensembles. The magnitude of the initial perturbation applied in these experiments has been shown in previous work with the 62 size-class configuration to be sufficiently small that the divergence of trajectories is independent of the magnitude of the initial perturbation (see Baird, in press; Lorenz, 1968).

To investigate the effect of the number of linkages on the growth of initial condition errors, ensembles of the 62 size-class configuration with the same magnitude perturbations as given above are run with the maximum size difference between predators and prey for both the protozoan and metazoan size-classes altered by a factor of 0.5, 1 (unaltered), 2, 3, and 4. Note that the 4× ensemble was terminated at 172 days because the tolerance of the adaptive Runge–Kutta failed to avoid negative plankton concentrations. Re-running all ensembles with a more stringent adaptive scheme was not practical. In any case the last 70 days of the 4× ensemble are not critical to the results presented.

For diagnostic purposes, for each ensemble, the number of interactions between size-classes are calculated. For the purpose of this calculation grazing between a predator and prey is counted as one interaction, although the term appears in two equations (one as a gain, and one as a loss). A second measure, the trophic position of predator *j*, TP_j , is calculated as the mean of the trophic position, TP_i of the n_j size-classes on which it preys, plus 1:

$$TP_j = \frac{\sum_{i=1}^{n_j} TP_i}{n_j} + 1 \quad (1)$$

where the trophic position of phytoplankton is one.

Two metrics are used to quantify divergence of trajectories, the ensemble spread from the control run (ESCR) and the ensemble spread from the ensemble mean (ESEM). ESCR is the mean distance between each perturbed member and the unperturbed control run.

ESEM is the mean distance between the each perturbed member and the mean of all perturbed members. For more information on these metrics see Baird (in press). Spread can be calculated for an individual variable, or summed for a group of variables, such as all phytoplankton size-classes, or indeed all biological variables.

In the experimental design the initial conditions errors are small, so all members of the ensemble, including the unperturbed control run, could be considered equally likely initial states. ESEM represents the ability of the ensemble mean to on average reduce the growth of initial condition errors. If ESCR is approximately equal to ESEM, then a single simulation is likely to have the same growth rate of initial condition errors as obtained using the ensemble mean. If ESCR exceeds ESEM, then on average the use of the ensemble mean reduces the growth of initial condition errors. Of course some of the perturbed members will be closer to the control run than the ensemble mean, and should have been preferred in a forecast to the ensemble mean, it is just not possible to predict which ones.

The analysis of model output requires configurations of different resolutions to be compared. It is not sensible to compare the biomass of the same size-class in all configurations, as in the higher resolution configurations this biomass will be expected to be spread among adjacent size-classes. To avoid this problem, the normalised biomass size spectrum (NBSS) is used (Platt and Denman, 1977). The NBSS is a plot of the biomass within a size interval divided by the width of the interval, against the width of the interval. As a result, the width of the interval can be changed (as a result of changing the number of size-classes) without changing the shape of the curve, allowing direct comparison of the size distribution of different resolution configurations. In practice the width is given by the distance between the midpoint either side of the considered size-class on a \log_2 scale.

4. Results

The general nature of the size-resolved pelagic ecosystem simulation is described in detail in Baird and Suthers (2007) and further analysed in Baird (in press). Briefly, the simulations are begun with an equal amount of biomass in each size-class. With a relatively constant physical forcing the pelagic ecosystem model is characterised by a series of predator–prey oscillations. The dominant oscillation in the 62 size-class configuration considered is between the phytoplankton size-class 8 ($r_p = 2.86 \mu\text{m}$) and its predators, which causes the period of greatest divergence of trajectories at around days 120–180. The model simulations are run for 240 days at which time the model has not approached an equilibrium state.

4.1. Effect of size-class resolution

Despite solving the same equations with the same parameter values, the number of size-classes alters the trajectories of the model (Fig. 4A–C). Increasing the number of size-classes results in the model trajectories following similar paths for longer (Fig. 4A–C). This convergence of behaviour with higher resolution is an indication of independence of the model equations on size-resolution of the integration. As shown in earlier work (Baird and Suthers, 2007), the total phytoplankton biomass in the 17 and 32 size-class configurations diverge from the other configurations at 25 and 75 days respectively. The 62 size-class configuration stays close to the finer resolution configurations until 125 days, before both deviating and incurring a large spread of ensemble members. The 123 configuration generally follows the 245 and 489 configurations. The 245 and 489 configurations have a small separation (mostly in time) between 50 and 100 days, but even they diverge strongly at 220 days. Later, when comparing divergence of members from

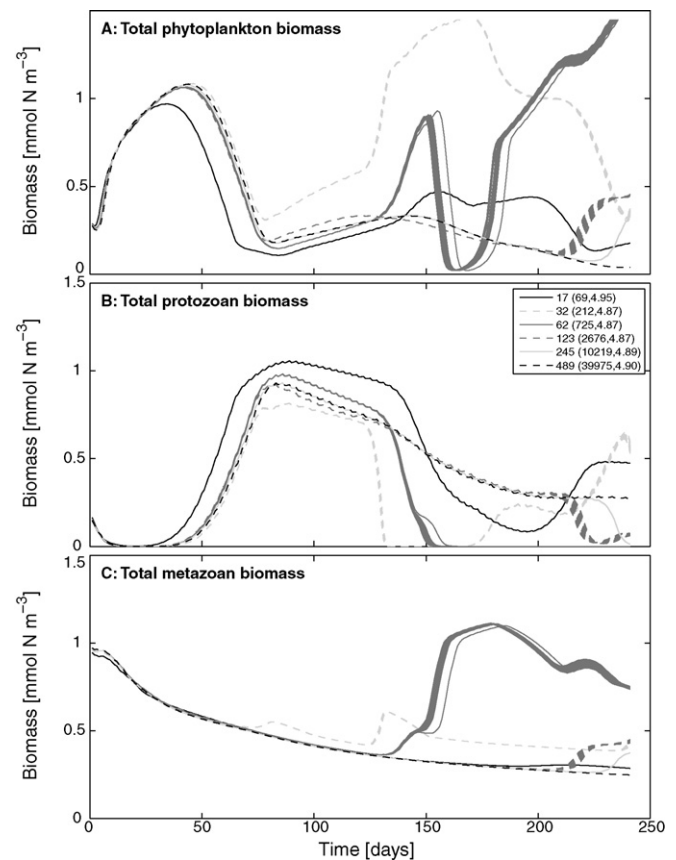


Fig. 4. Trajectories of (A) total phytoplankton biomass, (B) total protozoan biomass and (C) total metazoan biomass for the 17, 32, 62, 123, 245 and 489 size-class configurations. Each member of the each configuration is shown, although in most cases they plot on top of each other. Large spread is only visible for the 32 and especially the 62 size-class configurations.

different ensembles, it will be important to take into account the different states of the six configurations. Only the 123, 245 and 489 configurations are behaving in a similar manner between 120 and 200 days.

The divergence of size-class configurations affects not only the total biomass of phytoplankton, protozoan and metazoan groups, but also the size distribution within functional groups (Fig. 5). Initially all configurations have equal biomass in all size-class, with a slope of the normalised biomass size spectrum of -1 (not shown). After 30 days the spectra are still quite similar (Fig. 5A–C), although the coarseness of the 17 size-class configuration is becoming evident (Fig. 5C). By day 80, the 32 size-class configuration has a significantly different spectrum (Fig. 5D–F). The other classes, even the 17 size-class configuration, appear to be following that of the higher resolution configurations, albeit with the inevitable coarseness of their respective resolution. Between days 125 and 140 the 62 size-class configuration has moved towards small metazoans (Fig. 5L) outcompeting and/or consuming protozoans (Fig. 5K), resulting in a phytoplankton spectrum dominated by smaller phytoplankton (Fig. 5J). At day 140 the 123, 245 and 489 configurations still show similar size-distributions.

The effect of size-class resolution for very small perturbations in initial conditions is shown in Fig. 6. For the first 30 days, the ensemble spread from the control run of the 6 configurations is approximately equal. After 30 days, the greatest spread is seen in the 62 size-class configuration. With increasing resolution to 123 and 245 size-class configurations, spread decreases by an order of magnitude for each doubling of the resolution. Further increasing of the resolution to the 489 size-class configuration

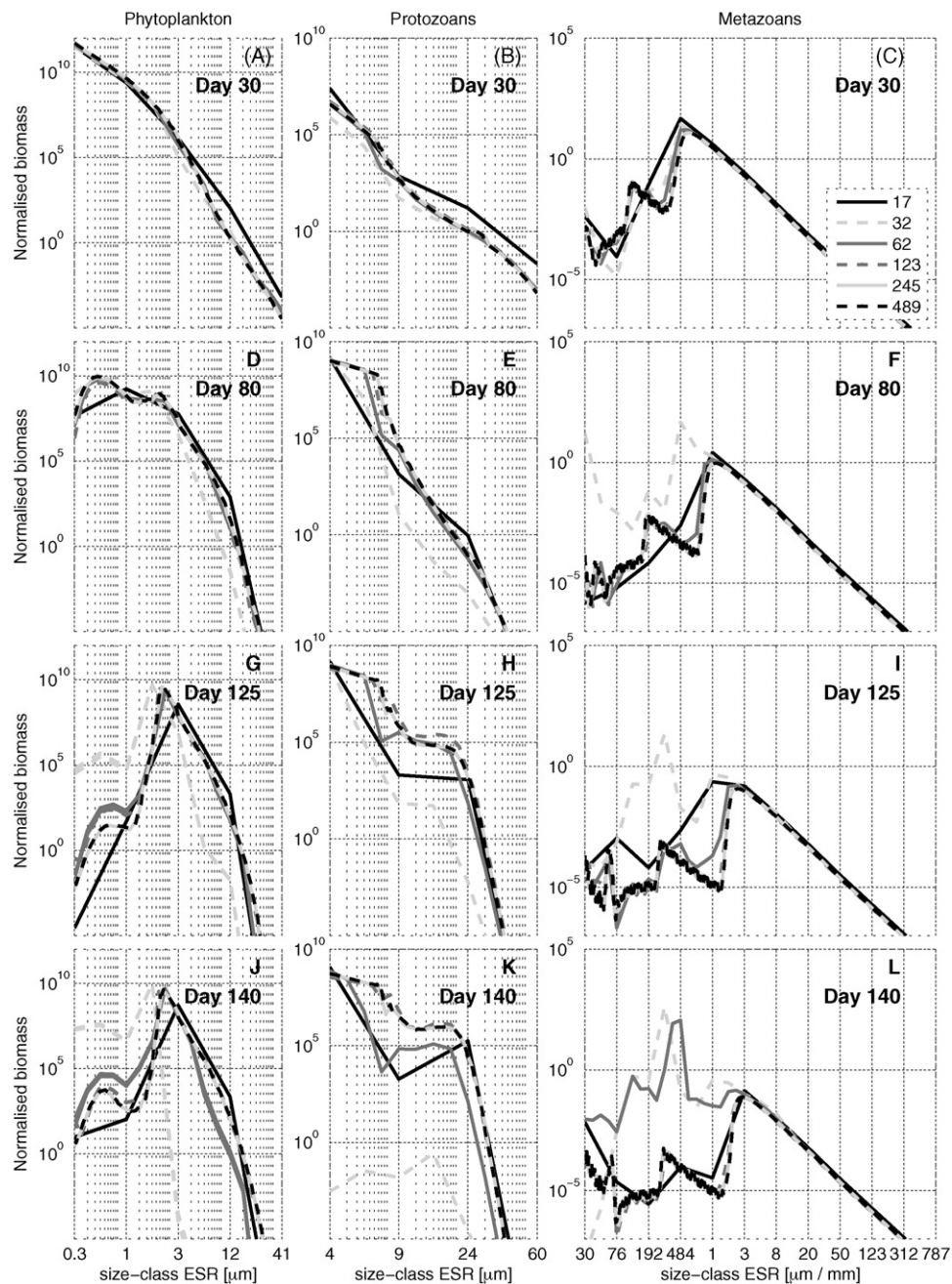


Fig. 5. Size distribution of all ensemble members of the six resolution configurations. The normalised biomass size spectrum is plotted for phytoplankton (left column), protozoans (centre column) and metazoans (right column) on days 30 (top row), 80 (2nd top row), 125 (third row) and 140 (bottom row) for the 17, 32, 62, 123, 245 and 489 size-class configurations (see legend of Panel C). The y-axis is biomass divided by the width of the size-class in mol N, and the x-axis is the size. For most spectra the ensemble members are similar, and only one line appears. The spread of an ensemble can be seen in the 62 and 245 size-class configurations in Panel G. The labelling of size-class uses equivalent spherical radius (ESR), and quantifies the largest eight metazoans in mm.

(the maximum that can logistically be undertaken at present) the spread is approximately unchanged from the 245 size-class configuration.

The 17 and 32 size-class configurations have reduced spread relative to the 62 size-class configuration. Fig. 4 shows that the 17 and 32 size-class configurations evolve in time differently to the 62, 123, 245 and 489 size-class configurations. Baird and Suthers (2007) found the reason for this different behaviour is poorly resolved predator–prey ranges. As a result of the different behaviour of the 17 and 32 configurations we will confine our understanding of the effect of resolution to analysis of the 62 and above size-class configurations in which model states are similar.

The output of the six size-class configurations has been reanalysed using the ensemble spread from ensemble mean (ESEM), and compared to the ensemble spread from the control run (ESCR). Initially ESEM is approximately twice the value of ESCR (Fig. 7). For a perturbation of 1 in an n member ensemble, initially the spread from the control run will be 1 for each member, or n for the whole ensemble. For calculating ESEM, the ensemble mean is $1/n$ more than the control for the perturbed variable, so the spread from the ensemble mean of the perturbed variable is $1 - 1/n$. Additionally the ensemble mean is $1/n$ removed for each unperturbed variable, so for n members, ESEM is initially $(1 - 1/n + (1/n)n)n$ or $2n - 1$. For large n , ESEM is

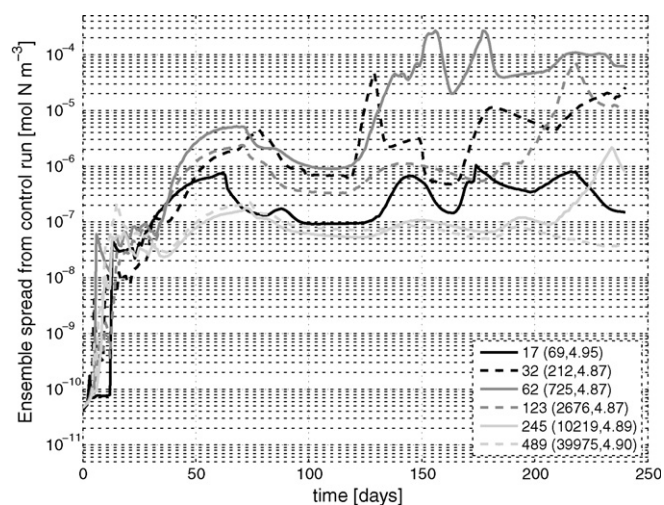


Fig. 6. Ensemble spread from control run of the biological state variables for the 17, 32, 62, 123, 245 and 489 size class configurations. The bracketed numbers in the legend give the number of interactions and maximum trophic position for the respective configurations.

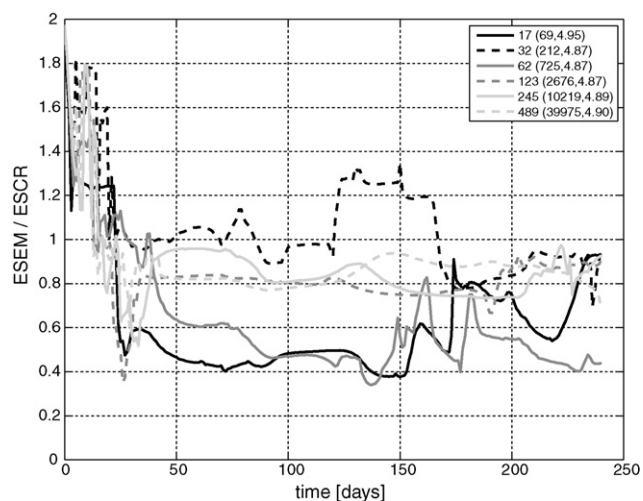


Fig. 7. The ratio of ensemble spread from the ensemble mean (ESEM) and ensemble spread from the control run (ESCR) of the biological state variables for the 17, 32, 62, 123, 245 and 489 size class configurations. See Fig. 6 for more details.

initially approximately $2n$. This effect quickly diminishes, and by day 20 ESEM is generally less than ESCR, or $ESEM/ESCR < 1$.

The ratio of ESEM/ESCR increases from the 62 size-class to the 123, while the ratio for the 245 and 489 size-classes is relatively equal (Fig. 7). The smaller ESEM/ESCR, the more the growth of initial condition errors is being overcome through the use of an ensemble. As shown above, the growth of initial condition errors is less in the 245 and 489 size-class configurations, and correspondingly, the use of an ensemble of simulations achieves a smaller reduction in error growth.

4.2. Effect of prey ranges

Increasing the prey range increases the number of interactions in the model as more prey are available to each predator, but decreases the maximum trophic level because on average each grazing interaction moves biomass further up the size spectrum (see legend of Fig. 8). Unlike the changes in the number of size-classes in the high resolution (62, 123, 245 and 489) configura-

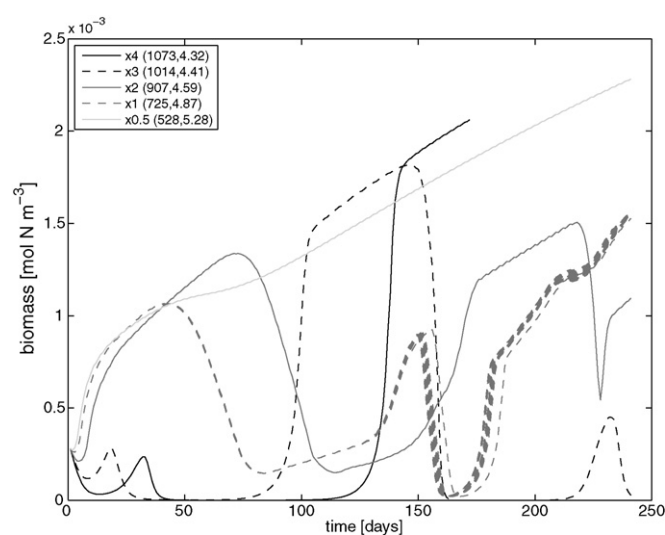


Fig. 8. Trajectories of total phytoplankton biomass for the 62 size-class configuration with the maximum size ratio between predators and prey alter by a factor of 0.5, 1 (unaltered) 2, 3, and 4.

tions, changing the maximum size difference between predators and prey changes the ecosystem that is being represented (Fig. 8). As a result, it is not possible to be clear on what fraction of the growth of initial condition errors is due changes in model structure alone, and what fraction is due to the interaction of changes in model structure and model state.

The effect of increasing maximum size difference between predators and prey on growth of initial condition errors is shown in Fig. 9. Decreasing the maximum size difference between predator and prey size-classes ($0.5\times$ case) results in ensemble spread levelling off at 10^{-7} mol N m $^{-3}$ after 100 days. The same occurs for the $0.25\times$ case (not shown). This occurs because with short prey ranges the smallest phytoplankton class has no predators, and the ecosystem is meaningless. Examining the case of increased prey ranges (from $1\times$ to $2\times$, $3\times$ and $4\times$), it is clear that increasing the prey range reduces ensemble spread. In contrast to the effect of size-class resolution, the effect of changing prey ranges has an immediate effect on member divergence. In the case $4\times$, there is virtually no spread, and the non-linear behaviour has been strongly damped.

As with the changing of the number of size-classes, increasing structural complexity, in this case by increasing prey ranges, inhibits the growth of initial condition errors.

5. Discussion

The numerical experiments undertaken in this paper show that for the size-resolved pelagic ecosystem model, increasing model structural complexity through increasing size-class resolution (for the same model equations and parameter estimates) decreases the divergence of trajectories. For model runs where the growth of initial conditions errors is the largest source of error, increased size-class resolution improves predictive skill.

It is inevitable that as resolution increases, the predictive skill of the model must eventually plateau, as is found in the similarity between the spread of the 245 and 489 size-class configurations. Were this not the case real world systems, which in one sense are infinitely resolved, would not undergo divergence from similar model states and chaotic behaviour would not be observed. It appears the 245 and 489 size-class simulations are close to the minimum divergence of the pelagic ecosystem model as used for these simulations (i.e. for the set of specified model equations, parameter values, and forcing functions).

It is sobering to consider that a model which is based on the same set of equations and parameter values, behaves so differently at different resolutions. Only the 245 and 489 size-class configurations show similar behaviour for the first 200 days. Does this mean 245+ size-classes are required for a 200-day forecast? Yes, if the purpose of the model is to capture the planktonic transients, or ‘plankton weather’ (but see Section 5.2). If the purpose of the model is at a longer time scale, or a more integrated understanding (i.e. primary and secondary production), which could be considered analogous to climate modelling, initial conditions become less important, and attraction to equilibrium states will cause trajectories to converge. Thus, if the steady-states are independent of resolution (this will be investigated in a future work), the high resolution models may not be required.

The divergence of members of an ensemble due to the growth of small initial condition perturbations is one source of error in a forecast. Others include, but are not limited to, errors in parameterisation, parameter values, forcing functions, boundary conditions, numerical approximations and missing processes. In ecological modelling much more so than atmospheric or hydrodynamic modelling, these sources of error are likely to be greater than those caused by non-linear feedbacks. As a result, [Fulton et al. \(2003\)](#) concludes that an intermediate level of model complexity is often more effective for forecasting purposes than a highly complex model. Nonetheless, in ecological modelling it is common for the model to be developed, and for the analysis to focus on understanding the model. Reducing growth of errors in initial conditions is useful, especially in single member runs, as it gives more confidence in the explanation of any particular simulations, which is inevitably based on a given set of initial conditions, model equations and parameter values. Additionally, short duration numerical modelling exercises, such as a phytoplankton bloom following coastal upwelling ([Baird et al., 2006](#)), depend more on initial conditions than parameterisations that determine steady-states. Under these circumstances, growth of initial condition errors are important.

5.1. Mechanism for inhibition of initial condition errors

The mechanism for the reduction in initial condition error growth in higher resolution configurations after 30 days is difficult to isolate, but a few comments can be made. Consider, for example, grazing, which is proportional to the concentration of a predator, Z , and a prey, P . The grazing term plus error will be proportional to $(P + \epsilon^P)(Z + \epsilon^Z) = PZ + P\epsilon^Z + Z\epsilon^P + \epsilon^Z\epsilon^P$, where ϵ^P and ϵ^Z are the differences between the predator, Z , and prey, P , of the ensemble member and the control run respectively. The grazing term error alone becomes proportional to $P\epsilon^Z + Z\epsilon^P + \epsilon^Z\epsilon^P$. Changing resolution by a factor of say 2 changes $P\epsilon^Z$, $Z\epsilon^P$, and $\epsilon^Z\epsilon^P$ by a factor of 4, but the total number of interactions is also changes by 4. A similar calculation for other interaction terms suggests that error growth for the individual processes should be not directly affected by a change in resolution.

Between 30 days and 80 days, the ensemble spread from control of the 62 size-class configuration becomes 5 times greater than the 123 size-class configuration, and a further order of magnitude greater than the 245 and 489 size-class configurations. On day 80, both the total biomass ([Fig. 4](#)), and size distributions of phytoplankton ([Fig. 5D](#)), protozoan ([Fig. 5E](#)) and metazoan ([Fig. 5F](#)) spectra in the 62, 123 and 245 size-class configurations are similar. Thus inhibition of the growth of initial condition errors between days 30 and 80 in the higher resolution configurations ([Fig. 6](#)) is not due to an artefact of changing biomass or size-distribution between configurations.

A breakdown of the contribution of each size-class in the 62, 123, 245 and 489 configurations to the divergence and conver-

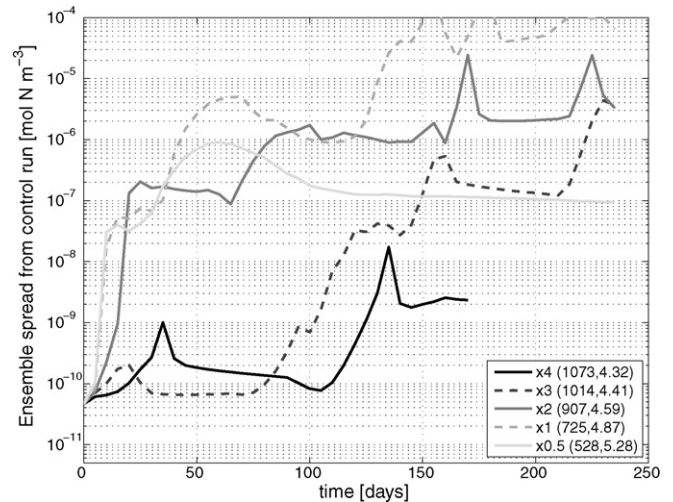


Fig. 9. Ensemble spread from control run of the biological state variables for the 62 size-class configuration with the maximum size ratio between predators and prey alter by a factor of 0.5, 1 (unaltered) 2, 3, and 4.

gence of the system is given in [Fig. 10](#) for days 75–85. The contributions are calculated as the component each size-class make to the Lyapunov exponent (see [Baird, in press](#) for calculation of Lyapunov exponent). The size-classes are quantified on the x-axis by their maximum growth rate, as a means of comparing their potential for growth driven divergence with the realised divergence. In the case of large metazoans, divergence is above that which could be achieved through growth. For these large metazoans, the mechanism of divergence is different rates of loss through grazing. The most significant result from this analysis is that the difference between the configurations of the divergence/convergence occurs primarily in the divergence ([Fig. 10A](#) has a clearer separation of configurations than [Fig. 10B](#)). Furthermore, it is fast growing metazoans in the 62 size-class configuration and protozoans in the 123 size-class that have anomalously high divergences that lead to the greater growth rate of initial condition errors.

In the search for a mechanism of error growth inhibition, it is possible to conclude: (1) the observed inhibition of the growth of initial conditions errors with increasing size-resolution between the 62 and 489 size-class configurations is not caused by a direct change in the biomass size-distribution, or a linear response in the plankton interaction terms; and (2) error growth is controlled by the divergence (rather than lack of convergence) of fast growing plankton. This is not the mechanistic description that we would like to grasp. It may be that the complex nature of non-linear feedbacks make these mechanisms difficult to isolate. In a somewhat similar study, [Chen and Cohen \(2001\)](#) showed effects of the number of species on amplitude of transients in Lotka–Volterra models. Other than correlations with the number of species or links (analogous to resolution here), they were not able to provide a mechanistic understanding or analytical result to explain the finding. In highly complex models mechanisms may be difficult to establish.

5.2. What does resolution mean in an ecological context

Model resolution, or the number of size-classes, does not correspond to standard ecological metrics. With increasing resolution, adjacent size-classes become more similar in their properties. In this sense, the resolution of the model is not a measure of biodiversity. The overall diversity of classes has not changed. Model resolution is also not a measure of individuals

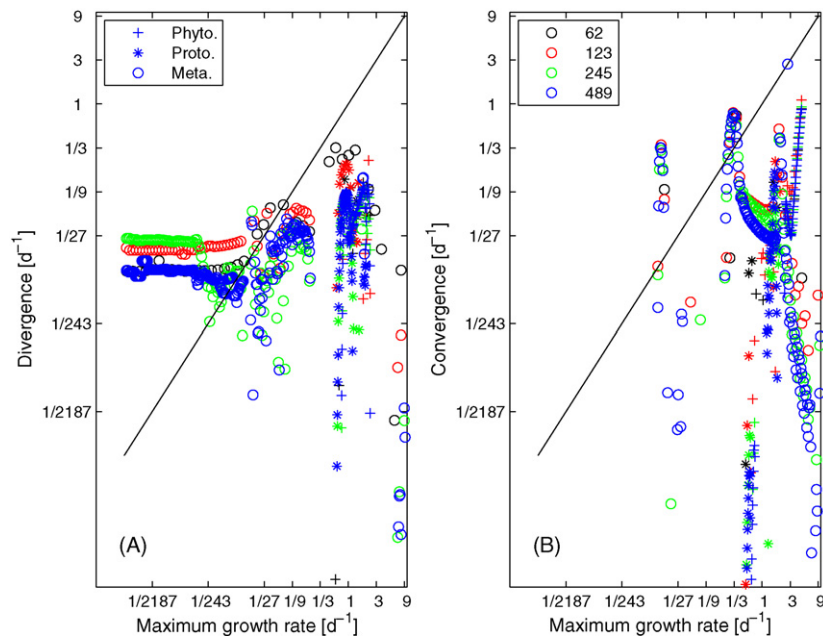


Fig. 10. The contribution to divergence (A) and convergence (B) of the phytoplankton (○), protozoan (*) and metazoan (+) size-classes during time periods 75–85 days for the 62 (black), 123 (red), 245 (green) and 489 (blue) size-class configurations. The x-axis is the maximum growth rate of the size-class, and the y-axis is the exponential rate of divergence (or convergence) of the size-class among ensemble members. Axes are log–log, with powers of 3 shown for reference.

within a population. Instead, as resolution gets finer, there are on average less individuals in a size-class, or population. Model resolution, as presented here, is a property of the model, in the same sense that the spatial resolution of a hydrodynamic model is a property of a model, rather than the water body being modelled.

In hydrodynamic modelling, a higher resolution model is generally considered to be a better model. This is not necessarily the case for an ecosystem model. While the model does converge at higher resolution this is not necessarily convergence on the most representative ecosystem. For a freshwater lake with only a limited number of phytoplankton species, the best number of classes to represent in the model is the number present in the lake. Over-representing for example, phytoplankton size-classes in the model may, as illustrated by Fig. 4, result in significant deviations from the ecosystem behaviour that is observed. On the other hand, size-distributions in fish data, which inevitably target a species, have been shown to fractal (García-Gutiérrez et al., 2009). So perhaps higher resolution may be a reasonable representation of size distributions within a species as well as across species.

It is worth noting that in this paper we have considered structural complexity to be calculated based on potential linkages between size-classes. This is a simple and easily interpretable metric. A more elaborate calculation could include a biomass-weighting to the connectance and trophic level metrics (or for another interesting alternative see Azovsky, 2009). In any case, for the consideration of structural complexity during model development, the measures used here are easy to interpret.

5.3. Minimising growth of initial condition errors

A comparison of the ensemble spread from the control simulation, and that from the ensemble mean provides a method of assessing the most effective method for reducing the growth of initial condition errors. The increase in resolution from 123 to 245 reduces the growth of initial condition errors by a factor of 5 (Fig. 6). The spread of the 75 member ensemble from the ensemble mean (ESEM) for the 123 and 245 configurations is at best 20% less than the spread from the control run (Fig. 7). Doubling the

resolution at four times the computational cost for a factor of five reduction in error growth is to be preferred over completing a 75 member ensemble, at 75 times the cost, for a 20% reduction in error growth. Such a decision, however, should consider other benefits of ensemble simulations, especially the ability to produce a probability density function for the evolving state of the system (Buizza et al., 2007).

In a spatially resolved pelagic ecosystem model not all regions will have moved equal distances in state space from initial conditions. For example, water close to an inflowing boundary will not have evolved far from the boundary condition. Perhaps more importantly for pelagic ecosystems, recently upwelled water, with concentrations that may be close to a climatological mean for deep water, will have departed less from initial conditions than a volume of water which has been in the euphotic zone for the duration of the simulation. As a result, it might be expected that growth of initial conditions errors is more likely to reduce predictive skill in the offshore, oligotrophic ocean than in near shore, productive regions.

The maximum size ratio between predator and prey will vary significantly between ecosystems, and within ecosystems due to changing seasons or external factors. An example of this is the widespread occurrence of salp blooms (Phylum Chordata, Class Thaliacea, Order Salpida). The most common species of salp off southeast Australia, *Thalia democratica* (Thompson, 1948) is approximately 1 cm in length, but consumes phytoplankton and bacteria up to seven orders of magnitude smaller (Andersen, 1998). In contrast, typical copepod predator prey ratios are approximately up to two orders of magnitude (Hansen et al., 1997). The numerical experiments undertaken in this paper suggests that the growth of initial condition errors will affect the predictive skill of ecosystems with a classic copepod-based food web more than those dominated by salps.

5.4. Implications for predator–prey modelling.

The non-linear behaviour of the size-resolved pelagic ecosystem model occurs as a result of predator–prey interactions, and the

general findings of this paper may be applicable to other predator–prey systems. The predation terms in the model are a linear function of encounter rate (which is itself a linear function of prey density) up until a physiological limit, as specified by a maximum growth rate of the predator (Baird and Suthers, 2007). This form is similar to saturated Lotka–Volterra grazing functions used in a variety of ecological models.

The pelagic ecosystem is particularly conducive to the numerical experiments investigated in this paper because the resolution of the model can be increased while using the same model equations and parameter values. This is made feasible with the assumptions that (1) all physiological processes can be quantified using an allometric relations; (2) all grazing interactions are based on size alone; and (3) that predators are always bigger than their prey. With these assumptions it is shown that increased model structural complexity inhibits the growth of initial condition errors. It would be more difficult to investigate structural complexity alone without these assumptions. Increasing resolution would tend to add new model parameterisations that blur the effect of increased structural complexity. Nonetheless, the results from the size-resolved pelagic ecosystem may be more broadly applied. That is, all other effects being small, increasing model structural complexity of predator–prey systems reduces the growth of initial condition errors, increasing the predictive capabilities of the model.

6. Summary

The ability to predict future states of pelagic ecosystems, and probably other ecosystems dominated by predator–prey dynamics, is a function of the number of biological classes resolved in the numerical model and the connectiveness of the classes. As a result of strong allometric trends, the effect of model complexity in pelagic ecosystems can be investigated without confounding factors such as the inclusion of additional parameterisation in more complex model structures. Numerical experiments show that after an initial period of equal divergence of model states, increasing structural complexity through increasing the number of size-classes inhibits the growth of initial condition errors. The rate of reduction of the growth of initial condition errors plateaus at high resolution. In cases where growth of initial condition errors is the greatest source of model error, structurally complex models are likely to outperform simple models.

Acknowledgements

This research was funded by ARC Discovery Project DP0557618. We thank Alan Blumberg and George Mellor for the free availability of the Princeton Ocean Model and Peter Oke for the physical configuration. We are particularly grateful to Duncan Smith, Martin Thompson and Michael Jansen for their engineering of the condor cluster, and the staff and students of the School of

Mathematics and Statistics on whose idle desktop computers the ensemble simulations ran. This paper arose to answer questions posed by Richard Matear and John Parslow during MB's extended visit to the CSIRO Hobart Laboratories.

References

- Andersen, V., 1998. Salps and pyrosomid blooms and their importance in biogeochemical cycles. In: Bone, Q. (Ed.), *The Biology of Pelagic Tunicates*. Oxford University Press, pp. 125–137.
- Azovsky, A.I., 2009. Structural complexity of species assemblages and spatial scale of community organization: a case study of marine benthos. *Ecol. Complexity* 6, 308–315.
- Baird, M.E., in press. Limits to prediction in a size-resolved pelagic ecosystem model. *J. Plankton Res.*
- Baird, M.E., Suthers, I.M., 2007. A size-resolved pelagic ecosystem model. *Ecol. Model.* 203, 185–203.
- Baird, M.E., Timko, P.G., Suthers, I.M., Middleton, J.H., 2006. Coupled physical-biological modelling study of the East Australian Current with idealised wind forcing. Part I. Biological model intercomparison. *J. Mar. Syst.* 59, 249–270.
- Buizza, R., Bidlot, J.-R., Wedi, N., Fuentes, M., Hamrud, M., Holt, G., Vitart, F., 2007. The new ECMWF VAREPS (Variable Resolution Ensemble Prediction System). *Q. J. R. Meteorol. Soc.* 133, 681–695.
- Chen, X., Cohen, J.E., 2001. Transient dynamics and food-web complexity in the Lotka–Volterra cascade model. *Proc. R. S. Lond. B* 268, 869–877.
- Duffy, J.E., Cardinale, B.J., France, K.E., McIntyre, P.B., Thebault, E., Loreau, M., 2007. The functional role of biodiversity in ecosystems: incorporating trophic complexity. *Ecol. Lett.* 10, 522–538.
- Fulton, E.A., Smith, A.D.M., Johnstone, C.R., 2003. Effect of complexity on marine ecosystem models. *Mar. Ecol. Prog. Ser.* 253, 1–16.
- Fussmann, G.F., Heber, G., 2002. Food web complexity and chaotic population dynamics. *Ecol. Lett.* 5, 394–401.
- García-Gutiérrez, C., Martín, M.A., Rey, J.-M. On the fractal modelling of biomass distributions: an application to size class in fisheries. *Ecol. Complexity* 6, 2446–253.
- Hansen, P.J., Bjornsen, P.K., Hansen, B.W., 1997. Zooplankton grazing and growth: Scaling within the 2–2,000 μm body size range. *Limnol. Oceanogr.* 42, 687–704.
- Hastings, A., 2004. Transients: the key to long-term ecological understanding? *Trends Ecol. Evol.* 19, 39–45.
- Hilborn, R.C., 2004. Sea gulls, butterflies, and grasshoppers: A brief history of the butterfly effect in nonlinear dynamics. *Am. J. Phys.* 72, 425–427.
- Huisman, J., Weissing, F.J., 2001. Fundamental unpredictability in multispecies competition. *Am. Nat.* 157, 488–494.
- Jackson, G.A., 1995. Coagulation of marine algae. In: Huang, C.P., O'Melia, C.R., Morgan, J.J. (Eds.), *Aquatic Chemistry: Interfacial and Interspecies Processes*. American Chemical Society, Washington, DC, pp. 203–217.
- Lorenz, E.N., 1963. Deterministic non-periodic flow. *J. Atmos. Sci.* 20, 130–141.
- Lorenz, E.N., 1968. The predictability of a flow which possesses many scales of motion. *Tellus* 21, 289–307.
- MacArthur, R.H., 1955. Fluctuations of animal populations, and a measure of community stability. *Ecology* 33, 533–536.
- May, R.M., 1973. *Stability and complexity in model ecosystems*. Princeton, Princeton.
- Melbourne, B.A., Hastings, A., 2009. Highly variable spread rates in replicated biological invasions: Fundamental limits to predictability. *Science* 325, 1536–1538.
- Platt, T., Denman, K., 1977. Organisation in the pelagic ecosystem. *Helgoländer Wiss. Meeresunters* 30, 575–581.
- Rai, V., Anand, M., Upadhyay, R.K., 2007. Trophic structure and dynamical complexity in simple ecological models. *Ecol. Complexity* 4, 212–222.
- Thompson, H., 1948. *Pelagic Tunicates of Australia*. CSIRO, Melbourne.
- Tilman, D., 1999. The ecological consequences of changes in biodiversity: a search for general principles. *Ecology* 80, 1431–1451.
- Wilder, J.W., 2001. Effect of initial condition sensitivity and chaotic transients on predicting future outbreaks of gypsy moths. *Ecol. Mod.* 136, 49–66.